Journal of Applied Physics ARTICLE scitation.org/journal/jap

SOL-GEL α-Al_2O_3 samples: Analysis of the TL kinetics

Cite as: J. Appl. Phys. **125**, 185102 (2019); doi: 10.1063/1.5088139
Submitted: 8 January 2019 · Accepted: 18 April 2019 ·
Published Online: 8 May 2019

Ivón Oramas Polo,[a] Danilo Oliveira Junot,[b] and Linda V. E. Caldas[c]

AFFILIATIONS

Instituto de Pesquisas Energéticas e Nucleares/Comissão Nacional de Energia Nuclear, IPEN/CNEN, Av. Prof. Lineu Prestes, 2242, 05508-000 São Paulo, SP, Brazil

[a]ivonoramas67@gmail.com
[b]dan.junot@gmail.com
[c]lcaldas@ipen.br

ABSTRACT

The analysis of the thermoluminiscence (TL) kinetics parameters of SOL-GEL α-Al_2O_3 with several different concentrations of impurities prepared through the solgel process is reported. A TL glow curve measured at 0.2 K/s after beta irradiation to 0.5 Gy revealed one peak at approximately 447 K. TL spectra were acquired and showed luminescent emission bands around 420 nm and 750 nm. The activation energies, the frequency factors, and the kinetic order involved in the TL emission were evaluated using the maximum peak temperature response, the peak shape of the TL glow curve, the TL glow curve area, and the glow curve fitting methods. The order of kinetics of the peak was evaluated as first order using T_M dependence on the radiation dose. The (T_M–T_{stop}) technique was used for determining the number of peaks in the glow curve. The activation energies obtained are in agreement with all the applied methods. The activation energy calculated by various methods varied from 0.885 ± 0.008 eV to 1.05 ± 0.10 eV. The frequency factor determined by all methods was of the order of 10^9 s^{-1}. The dosimetric peak is affected by thermal quenching. The following thermal quenching parameters were estimated: the activation energy of the thermal quenching $W = 1.05 \pm 0.15$ eV and the constant $C = 8.27 \times 10^{10}$ s^{-1}. The trapping parameters of SOL-GEL α-Al_2O_3 detectors are reported in the present work for the first time.

I. INTRODUCTION

In 1950, the use of undoped Al_2O_3 was already suggested for TL dosimetry. In 1990, Russian scientists were able to increase the sensitivity of this material with the introduction of high concentrations of oxygen vacancies. The introduction of carbon into the crystal contributed to the formation of the F and F+ luminescence centers. Due to the high TL sensitivity of this material, 40–60 times greater than that of LiF TLD-100 (Akselrod *et al.*, 1990), it can be used in low dose dosimetry. There are several chemical methods for the synthesis and production of aluminum oxide, including precipitation, spray pyrolysis, organic precursors, Pechini, etc. (Jalali, 2018). These methods and the commercial well-established crystal growth technique are complex, sophisticated, and time-consuming procedures. These methods are not always easy to implement in a usual laboratory (De Azevedo *et al.*, 2006 and Jalali, 2018).

The synthesis of luminescent materials by the solgel process is a relatively low cost method for routine monitoring that can be implemented in a usual laboratory infrastructure. The difference between the solgel technique and the conventional high temperature synthesis processes is that solgel is a low temperature method, which uses chemical precursors to produce materials with better purity and homogeneity (Brinker and Scherer, 1990 and Rivera, 2011). The solgel process is a method that allows high reproducibility, and its synthesis can easily be adapted from a laboratory production to large-scale production (Ferreira and Santos, 2014). The application of the solgel technique in the synthesis and characterization of the thermoluminescent materials has been discussed in several works (Rivera *et al.*, 2006; 2007a; 2007b; 2010; and Bao *et al.*, 2007). The solgel process has been successfully used for the synthesis of a large number of mono metal oxide phases (Al_2O_3, TiO_2, ZrO_2, etc.) (Rivera *et al.*, 2007b). Aluminum oxide has been synthesized and

produced by the solgel process for dosimetric purposes (Pierre, 1998 and Bitencourt *et al.*, 2010).

The SOL-GEL α-Al_2O_3 detectors were prepared through the solgel process followed by calcination, pressing, and sintering in a highly reducing atmosphere at the Centro de Desenvolvimento da Tecnologia Nuclear (CDTN/CNEN) in Belo Horizonte, Brazil. Aluminum nitrate dissolved in alcohol was used for the production of the SOL-GEL α-Al_2O_3 detectors as an alumina precursor. To this solution were added nitrates of metals used as dopants such as Fe, Mg, Ca, Cr, Ni, and Mo, as well as C. The detectors were tested in a ^{137}Cs gamma beam, and they showed good dosimetric characteristics, high sensitivity, good reproducibility, good batch homogeneity, and good linearity of response in a dose range of 0.01–1000 mGy. In order to improve the sensitivity of these detectors, impurities were added to some samples in their preparation. These samples showed a TL sensitivity three times higher than that in samples without these impurities (Ferreira and Santos, 2014).

To describe the TL process in the material, the glow curves are usually analyzed, and the trapping parameters, namely, the activation energy E, the frequency factor s, and the kinetic order b of the TL process, were determined (Pagonis *et al.*, 2006). Many methods have been proposed and applied for the evaluation of the kinetic parameters based on the analysis of the glow curves (McKeever, 1980; 1985; Chen and McKeever, 1997; Kitis *et al.*, 1998; Kitis, 2001; Furetta, 2003; Pagonis *et al.*, 2006; Chen and Pagonis, 2015; and Chen *et al.*, 2016).

Even if the Al_2O_3:C crystals present excellent dosimetric characteristics, they reveal significant variations in the shape of the TL glow curve. There may be found TL glow curves with a narrow, a wide, double, or several peaks in the temperature range between 130 °C and 270 °C (403 K–543 K). This diversity suggests a distribution of traps with different trapping parameters. This is related to the fact that the crystals are grown in different conditions and the impurities may change (Akselrod and Akselrod, 2002).

Although the glow curve can give information about the detrapping process that occurs in the material, the wavelength measurements give information about the different recombination process that takes place in that material (Chen and McKeever, 1997). The measurements of the light emitted at certain wavelengths during heating were taken with a spectrometer and the graph is known as a 3D TL plot: the TL intensity vs temperature and vs wavelength (Bos, 2017). These measurements are taken for research purposes with specific characteristics in materials. It is difficult to apply this configuration in the daily routine because the measurements are time-consuming (Chen and McKeever, 1997 and Yoshizumi and Caldas, 2014).

The effect of thermal quenching is present in several important materials, such as quartz and Al_2O_3 (Akselrod *et al.*, 1998; Kitis, 2002; Pagonis *et al.*, 2006; Chithambo, 2014; and Kalita and Chithambo, 2017a; 2017b). According to Furetta (2008), the effect of thermal quenching can be defined as "the process such that the luminescence efficiency decreases with temperature, due to the increased probability of nonradiative transitions due to killer centers." This effect was reported by the SOL-GEL α-Al_2O_3 producers as practically nonexistent on these detectors (Ferreira and Santos, 2014). However, it was noticed that with the increase of the heating rate, the area under the glow-peak decreases, and this fact suggests that probably the peak is affected by thermal quenching (Furetta, 2008 and Chithambo, 2014).

The determination of the kinetic parameters of the SOL-GEL α-Al_2O_3 polycrystalline detectors and the thermal quenching remained as subjects of further research. The material producer focused mainly on the material production conditions and on the dosimetric characteristics of these detectors (Ferreira and Santos, 2014). Although the kinetic parameters of Al_2O_3:C synthesized with other methods have already been studied, a detailed analysis of the kinetic parameters of aluminum oxide synthesized with the solgel method with several different concentrations of impurities has not been published yet. Therefore, the objective of this work was to analyze the TL kinetic parameters of SOL-GEL α-Al_2O_3 material for the first time and to investigate the effect of the thermal quenching in the dosimetric peak. Different methods of data analysis were evaluated.

II. MATERIALS AND METHODS

A. Characterization

The material analysis using inductively coupled plasma mass spectrometry (ICP-MS, ELAN DRC/PerkinElmer) revealed the following impurity content: Fe 99.8 ± 9.9 ppm, Mg 0.9 ± 0.10 ppm, Ca 310 ± 30.6 ppm, Cr 31.5 ± 3.2 ppm, Ni 25.0 ± 2.5 ppm, Mo 5.0 ± 0.3 ppm, and C 895.5 ± 44.8 ppm. After this phase, the material was dried, the powder was grown and calcinated in air atmosphere. After that, the powder was mixed with a polyvinyl alcohol solution, and then it was pressed into discs (Ferreira and Santos, 2014).

The SOL-GEL α-Al_2O_3 detectors have 4.59 ± 0.01 mm in diameter, 1.119 ± 0.010 mm in thickness, and 51.8 ± 0.4 mg of mass.

TL measurements were performed under an N_2 atmosphere in a RISØ TL/OSL-DA20 system. The detectors were irradiated using the ^{90}Sr/^{90}Y beta reader source with a dose of 0.5 Gy. The luminescence was detected by a bialkali EMI 9235QB photomultiplier tube (PMT) which has a maximum detection efficiency between 200 and 400 nm. The 7 mm band pass filter Hoya U-340 (transmission band 250–390 nm FWHM) was utilized (DTU Nutech, 2015). For the determination of the kinetic parameters, the heating rate was 0.2 K/s, and the maximum temperature was 623 K. The samples were thermally treated at 873 K for 30 min under the air atmosphere.

The TL emission spectra were measured using an Ocean Optics QE65 Pro spectrometer which provides enhanced response in the UV and short-wave near-infrared (SW-NIR). The detector used in the QE65 Pro spectrometer is a scientific-grade, back-thinned, TE Cooled (TEC), 1044 × 64 element CCD array from Hamamatsu. The detector spectral range is 200 up to 1100 nm with window (Ocean Optics, 2018). The optical fiber used was a UV–vis solarization-resistant fiber, with 1.0 mm core diameter. This fiber presents a relative transmission better than 80% in the range of 250–900 nm. TL spectra acquired were not corrected for the spectral sensitivity of the spectrometer.

When peaks of relatively high temperature are measured, the black body phenomenon may occur. A black body is an object that absorbs all radiation at all wavelengths. As the temperature decreases, the peak of the black body radiation curve moves to lower intensities and to the longer wavelengths. The black body

may cause a distortion in the TL peak shape. This can significantly reduce the accuracy of the measurement. This can be solved by using a filter in case where the TL emission is not in the red region, since the black body radiation occurs mainly in the red and infrared regions (Chen and Kirsh, 1981). In this work, the effects of this phenomenon were negligible, since the Hoya U-340 filter was used.

B. Kinetic parameters

The simplest model to explain the TL process consists of an electron trap (T) and one recombination center (RC). This model is known as OTOR (one-trap-one-recombination center). The traps capture electrons and the recombination centers capture holes. In the OTOR model, N is the total concentration of the traps in the crystal (m^{-3}), n is the concentration of filled traps in the crystal (m^{-3}) at time t, h is the concentration of trapped holes in the recombination center (m^{-3}), A_n is the retrapping probability of electrons ($m^{-3}\,s^{-1}$), A_{RC} is the recombination probability of electrons ($m^{-3}\,s^{-1}$), and n_0 is the initial concentration of filled traps at time $t = 0$. To obtain the equation that governs the TL process during heating, the following considerations are taken into account: the sample is heated following a linear function that varies linearly with time $T = T_0 + \beta t$, where β is the constant heating rate; the irradiation has ended; when the temperature of the sample increases, the trapped electrons are released into the conduction band, and they can recombine with holes in the recombination centers. The TL intensity is proportional to the recombination rate of holes and electrons in the recombination center,

$$I(t) = dh/dt. \tag{1}$$

For first order kinetics, the following assumptions are used: $n \cong h$, $\frac{dn}{dt} \cong \frac{dh}{dt}$, and $A_{RC}\,h \gg A_n(N-n)$. Taking into account these assumptions, the equation of first order kinetics is

$$I(t) = -dn/dt = nse^{-E/kT}. \tag{2}$$

For general order kinetics, the equation is

$$I(t) = -dn/dt = n^{b}{*}s'{*}e^{-E/kT}, \tag{3}$$

where E (eV) is the activation energy or depth of the trap and it is the energy associated with a metastable level within the crystal forbidden band; n is the concentration of trapped holes in the recombination center (m^{-3}), k is the Boltzmann constant (eV/K), T is the absolute temperature (K), b is the kinetic order (typically between 1 and 2), s is the frequency factor (s^{-1}), and s' ($m^{3(b-1)}\,s^{-1}$) is the effective pre-exponential factor for the general order kinetics (Pagonis *et al.*, 2006).

The general order kinetic equation is empirical, and s' is not constant with dose.

The individual peaks of the TL glow curve can be analyzed to determine the kinetic parameters: activation energy E, the attempt to escape frequency factor s, and kinetic order b. The activation energy and the frequency factor are called trapping parameters. The values of these parameters determine if the electron will escape at a given temperature (Bos, 2017). The integral of Eq. (1) has to be evaluated using numerical integration methods, but there are some alternative procedures that can be used (Furetta and Weng, 1998; Pagonis *et al.*, 2006; and Bos, 2017).

In order to determine the total number of peaks and their position in the glow curve, the known (T_M–T_{stop}) method was used (McKeever, 1980). This method consists of monitoring the position of the maximum glow curve temperature peak T_M. The method begins by irradiating a sample that is first heated at linear rate to a temperature corresponding to the initial rise of the first peak. The sample is then cooled quickly to room temperature and then reheated at the same linear rate to obtain the remaining glow curve. The position of the maximum T_M is recorded. This process must be repeated each time with a sample that has to be irradiated using T_{stop} values for each of their steps. The value of T_{stop} must be increased in small increments, and then the plot of T_M vs T_{stop} should be obtained. For the first order glow peak, the (T_M–T_{stop}) curve will be a line of null slope. For a glow curve that contains various separated first order peaks, the (T_M–T_{stop}) curve will have a characteristic "staircase" structure (McKeever, 1980).

One method used to evaluate the kinetic order of the peak is the T_M-dose method. It consists of irradiating the samples with different doses under the same experimental conditions. According to McKeever (1980), the position of the first order peak is independent of the dose at which the samples were irradiated.

In this work, several methods were used to determine the kinetic parameters. The methods are described.

C. Methods of analysis based on the maximum peak temperature

Randall and Wilkins (Pagonis *et al.*, 2006 and Furetta, 2008) considered that the temperature of the TL glow curve, in which the probability of an electron scape from the trap is equal to 1, is the maximum temperature. These authors used Eq. (4) to determine the activation energy considering $s = 2.9{*}10^9\,s^{-1}$,

$$E = 25kT_M. \tag{4}$$

According to Urbach, who considered $s = 10^9\,s^{-1}$ (Pagonis *et al.*, 2006),

$$E = 23kT_M. \tag{5}$$

These methods were used only as a first approximation of the activation energy values.

D. Methods of analysis based on the peak shape of the TL glow curve

In these methods, the kinetic parameters are determined based on the shape of the TL glow curve (Chen and McKeever, 1997; Furetta and Weng, 1998; Pagonis *et al.*, 2006; and Furetta, 2008). The parameters to be defined in these methods are represented in Fig. 1.

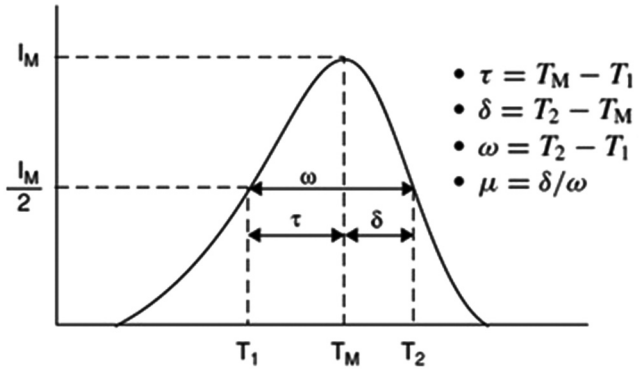

FIG. 1. Geometric parameters based on the shape of the TL glow curve (T_M: peak temperature at the maximum intensity; T_1, T_2: temperatures on either side of T_M, corresponding to the half intensity) (Pagonis *et al.*, 2006).

Next, some expressions to determine the activation energy for first order kinetic are presented (Furetta, 2008).

According to Grossweiner:

$$E = 1.51^{*}k^{*}(T_M T_1)/\tau. \tag{6}$$

According to Lushchik:

$$E = 0.976^{*}(k^{*}T_M^2)/\delta. \tag{7}$$

According to Halpering and Braner:

$$E = (1.59^{*}k^{*}T_M^2)/\tau - 3.16^{*}k^{*}T_M. \tag{8}$$

Equation (7) can be used to determine the activation energy, and it was proposed by Balarin (Furetta, 2008),

$$E = T_M^2/4998^{*}\omega. \tag{9}$$

Chen established an expression for general order kinetics (Furetta, 2008). The expression to determine the activation energy as a function of the factor μ is

$$E_\alpha = c_\alpha{}^{*}(k^{*}T_M^2/\alpha) - b_\alpha(2^{*}k^{*}T_M), \tag{10}$$

where α represents the parameters τ, δ, or ω. The values of c_α and b_α are

$$c_\tau = 1.51 + 3.0\,(\mu - 0.42), \quad b_\tau = 1.58 + 4.2\,(\mu - 0.42), \tag{11}$$

$$c_\delta = 0.976 + 7.3\,(\mu - 0.42), \quad b_\delta = 0, \tag{12}$$

$$c_\omega = 2.52 + 10.2\,(\mu - 0.42), \quad b_\omega = 0. \tag{13}$$

Once the activation energy has been determined, the frequency factor for first order kinetics can be estimated by the following equation:

$$s = \frac{\beta^{*}E}{kT_M}{}^{*}\exp(E/kT_M). \tag{14}$$

E. Methods of analysis using the TL glow curve area

These methods, known as "area methods" or "entire TL glow curve peak methods," are based on the measurement of the integral below the curve peak. The value of the integral $n(T)$ of the intensity TL can be estimated as the area from a temperature T_0 to a final temperature T_f at the end of the peak curve (Furetta and Weng, 1998; Pagonis *et al.*, 2006; and Furetta, 2008). The following equation is used for this method:

$$\ln(I(T)/n^b) = \ln s'/\beta - E/kT, \tag{15}$$

where β is the heating rate.

From Eq. (15), a graph of $\ln(I(T)/n^b)$ vs $1/kT$ can be plotted with several values of the kinetic order b. The graphs fit linearly, and the graph with the best R^2 coefficient corresponds to the best value of b. From these graphs, it is possible to determine the activation energy as the angular coefficient of the fitting line, and with the line intercept, the frequency factor can be determined from the following equation:

$$s = \beta^{*}e^{(intercept)}. \tag{16}$$

F. Curve deconvolution

The computer program GlowFit was used for the glow curve deconvolution. The GlowFit is a program for deconvoluting first order kinetic TL glow-curves. It is based on the first order kinetics model. A single glow-peak is described by a nonlinear function, and it is fitted to experimental values using an iterative Levenberg–Marquardt method. In the program report, a parameter describing the fitting quality, called Figure of Merit (FOM), is also presented,

$$\text{FOM}\ (\%) = \frac{\sum_i |y_i - y(x_i)|}{\sum_i y_i}{}^{*}100\%, \tag{17}$$

where y_i is the content of the channel and $y(x_i)$ is the value of fitting function in the middle of the channel (Puchalska and Bilski, 2006).

The program is freely downloadable from the website http://www.ifj.edu.pl/dept/no5/nz58/deconvolution.htm.

G. Analysis of thermal quenching

Due to the effect of thermal quenching, the area underneath the glow curve peak decreases with the increase of the heating rate (Pagonis *et al.*, 2006). The efficiency of the thermoluminescence $\eta(T)$ can be defined by the following equation:

$$\eta(T) = A_q/A_{uq} = 1/1 + C^{*}\exp(-W/k^{*}T_M), \tag{18}$$

where A_q and A_{uq} are the areas under the curves with and without the effect of the thermal quenching, respectively; W is the activation energy of the thermal quenching, and C is a constant (Pagonis *et al.*, 2006 and Kalita and Chithambo, 2017a).

According to the model of Akselrod *et al.* (1998), W is the potential barrier required for the thermal release of trapped holes that result in a decrease in the concentration of luminescent centers as the temperature increases. C is a dimensionless constant defined by the nonradiative transition probability ratio and the radiative transition probability (Pagonis *et al.*, 2010).

In order to obtain the W and C parameters, it is necessary to take measurements of the glow curves with different heating rates. Considering that the area of the glow curve with the lowest heating rate is A_{uq}, the curve of $\ln[(A_{uq}/A_q)-1]$ vs $1/kT_M$ should be plotted. This curve will produce a straight line with angular coefficient $-W$ and intercept $\ln(C)$, from which the parameter C can be evaluated (Pagonis *et al.*, 2006 and Kalita and Chithambo, 2017a).

III. RESULTS AND DISCUSSION

A. Thermoluminescence spectra

The TL spectra of SOL-GEL α-Al_2O_3 detectors as a function of temperature and the wavelength, recorded at 5 K/s by a spectrometer and an optical fiber, are shown in Figs. 2–5. The irradiation doses were 5 Gy, 10 Gy, 20 Gy, and 50 Gy, respectively, in order to obtain a well-defined signal to identify the recombination centers.

The spectra measured at 5 K/s after beta irradiation to 0.5 Gy revealed the peaks at approximately 420 nm, 697 nm, 750 nm, and 800 nm.

The dosimetric peak of SOL-GEL α-Al_2O_3 measured at 5 K/s appears at ∼508 K and ∼420 nm. This peak is characterized by a broad emission. According to some authors, this band coincides with emission bands in F center (oxygen vacancies with two electron captures), which produce luminescence (Yukihara *et al.*, 2003 and Akselrod *et al.*, 2006). Also probably, this emission, which appears in most aluminosilicates with different chemical compositions and variable order of Al and Si, may be attributed to the recombination that occurs in a center associated with the reticular defects of the type Al-O-Al or Si-O-Si (Valle *et al.*, 2004).

The infrared (IR) emission centered near 697 nm is attributed to the presence of Cr^{3+} in the crystal lattice (Lu *et al.*, 2013; Gaft *et al.*, 2015; and Nyirenda and Chithambo, 2018). Caiut *et al.* (2018) obtained spectra containing the well-known sharp R lines at 694 nm with the Cr^{3+}-doped alumina powder. Nyirenda and Chithambo (2018) reported that the peak intensity of Cr^{3+} decreases with increasing temperature. This decrease could be associated with the effects of thermal quenching (Bouman, 2016).

The emission at ∼750 nm may be associated with the presence of Mg 0.90 ± 0.10 ppm as impurity in the crystal of SOL-GEL α-Al_2O_3. Some authors reported that this band is due to F_2^+(2Mg) center (Akselrod and Akselrod, 2006; Rodriguez *et al.*, 2011; and Kalita and Chithambo, 2017b).

Figures 3–5 show the strong luminescence at 800 nm in all spectra for doses above 5 Gy. Some authors observed that the growth of crystals in atmospheres in the presence of oxygen leads to an increase in luminescence in the 800 nm band (Rotman *et al.*, 1989 and Varney *et al.*, 2011). These authors attribute the luminescence in the 700 and 800 nm emission bands to the presence of Fe^{3+} impurities for the following reasons: In many materials in the 700 nm and 1000 nm bands, the Fe^{3+} impurity has a broad emission; in materials doped with iron, luminescence peaks were observed at 800 nm, and the growth conditions in air atmosphere improved and increased the

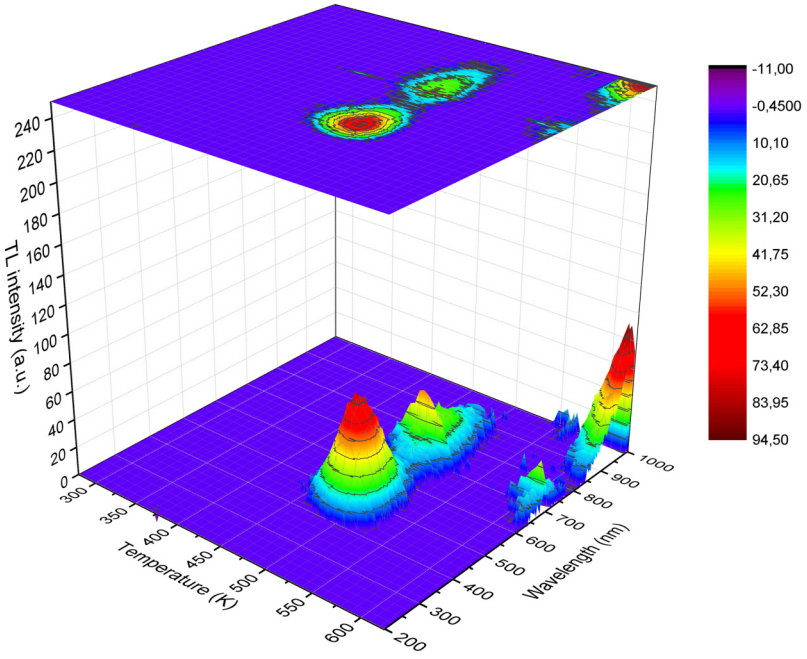

FIG. 2. TL emission spectrum of SOL-GEL α-Al_2O_3 irradiated with 5 Gy of beta radiation.

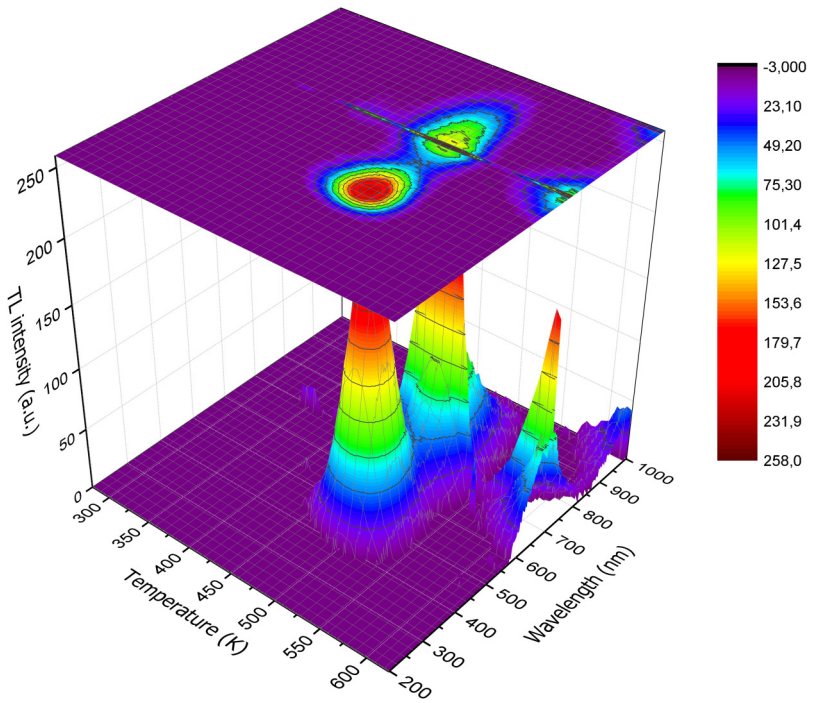

FIG. 3. TL emission spectrum of SOL-GEL α-Al_2O_3 irradiated with 10 Gy of beta radiation.

emission at the 700 nm and 800 nm bands. According to the analysis using ICP-MS by the producer, the iron impurity content was 99.8 ± 9.9 ppm (Ferreira and Santos, 2014). Probably, this level of iron causes that intense luminescence. According to Varney *et al.* (2011), oxygen vacancies are filled by air oxygen in the growth process, and they provide oxygen ligands near Fe^{3+}.

The TL intensity at high temperatures and long wavelengths is due to black body radiation (Bos, 2017).

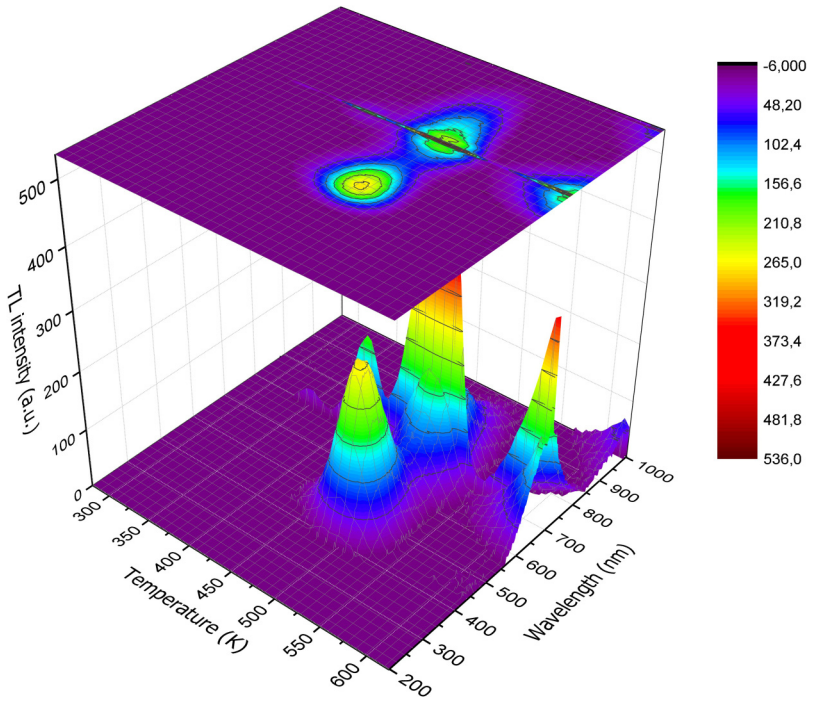

FIG. 4. TL emission spectrum of SOL-GEL α-Al_2O_3 irradiated with 20 Gy of beta radiation.

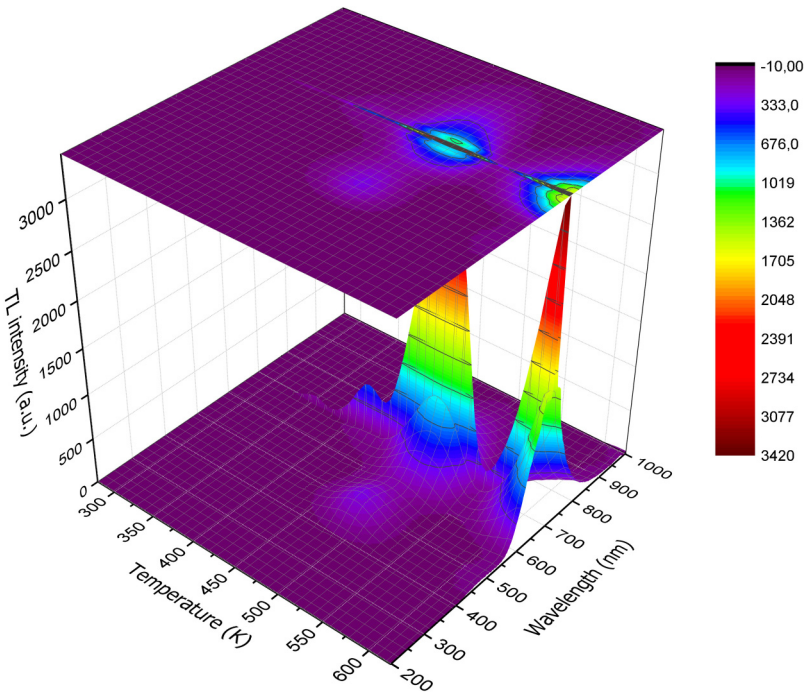

FIG. 5. TL emission spectrum of SOL-GEL α-Al_2O_3 irradiated with 50 Gy of beta radiation.

The filter most commonly used with the RISØ TL/OSL system is the Hoya U340 filter of 7.5 mm. This filter presents a high transmission peak (~80% at 340 nm) (DTU Nutech, 2015), but it allowed a low proportion of the SOL-GEL α-Al_2O_3 glow curve to be transmitted, because the filter window is centered at ~365 nm, and the detector emission is above 400 nm. As a result, most of the TL emission is ignored, especially that producing emission in the long wavelength region. In addition to the Hoya U340 filter, there are two types of filters with other characteristics. These filters are the following: Schott BG 39 of 1 mm and Corning 70-59 of 4 mm or BG3 of 1 mm. Figure 6 shows the transmission characteristics of the RISØ TL/OSL system filters.

In order to achieve a high transmission in the bands of SOL-GEL α-Al_2O_3 detectors, a filter or filter configuration should be selected to obtain a better TL emission. The use of different filters allows the increase in the measurement range. The combination of filters Schott BG3 and Schott BG39 would have an appropriate detection window for SOL-GEL detectors and give a detection efficiency of 65%. The combination of Corning 7-59 and Schott BG39 would also be appropriate, and the transmission efficiency would be about 60%. All the measurements were taken with the Hoya U340 filter, which is the standard filter that is available in the LCI/IPEN. Although a part of the TL emission is ignored with this filter, the GEL SOL detectors presented an adequate response and sensitivity to radiation (Polo and Caldas, 2019).

B. Thermoluminescence peak structure

One TL sample was irradiated to 0.5 Gy and its TL glow curve was obtained at 1 K/s. Due to the significant variations in the shape of the TL glow curve of the aluminum oxide (Akselrod and Akselrod, 2002), the measurements were taken after heating up the sample to certain temperature ranges, in order to detect the presence of temperature peaks. Figure 7 shows a partial heating experiment: (a) the sample was partially heated up to 413 K, and then the resulting glow curve was recorded. There were no peaks between 273 K and 413 K; (b) the sample was partially heated up to the temperature beyond the peak, and the resulting glow curve was recorded. The TL peak was around 470 K; (c) the sample was heated up to 623 K, and the resulting glow curve was recorded. There were no peaks between 502 K and 623 K; (d) sum of all the partial curves with the dosimetric peak.

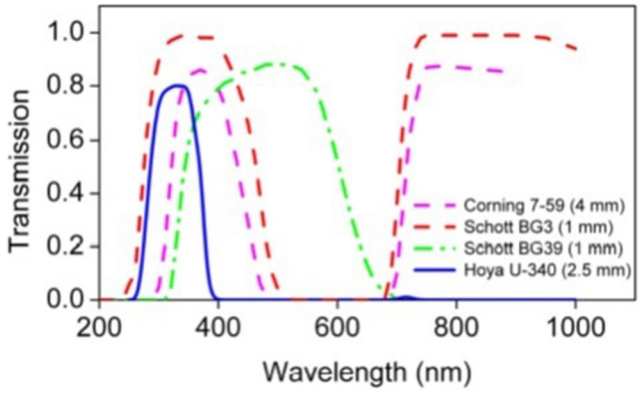

FIG. 6. Transmission characteristics of the detection filters Hoya U-340, Schott BG 39, and Corning 7-59 or Schott BG3) (DTU Nutech, 2015).

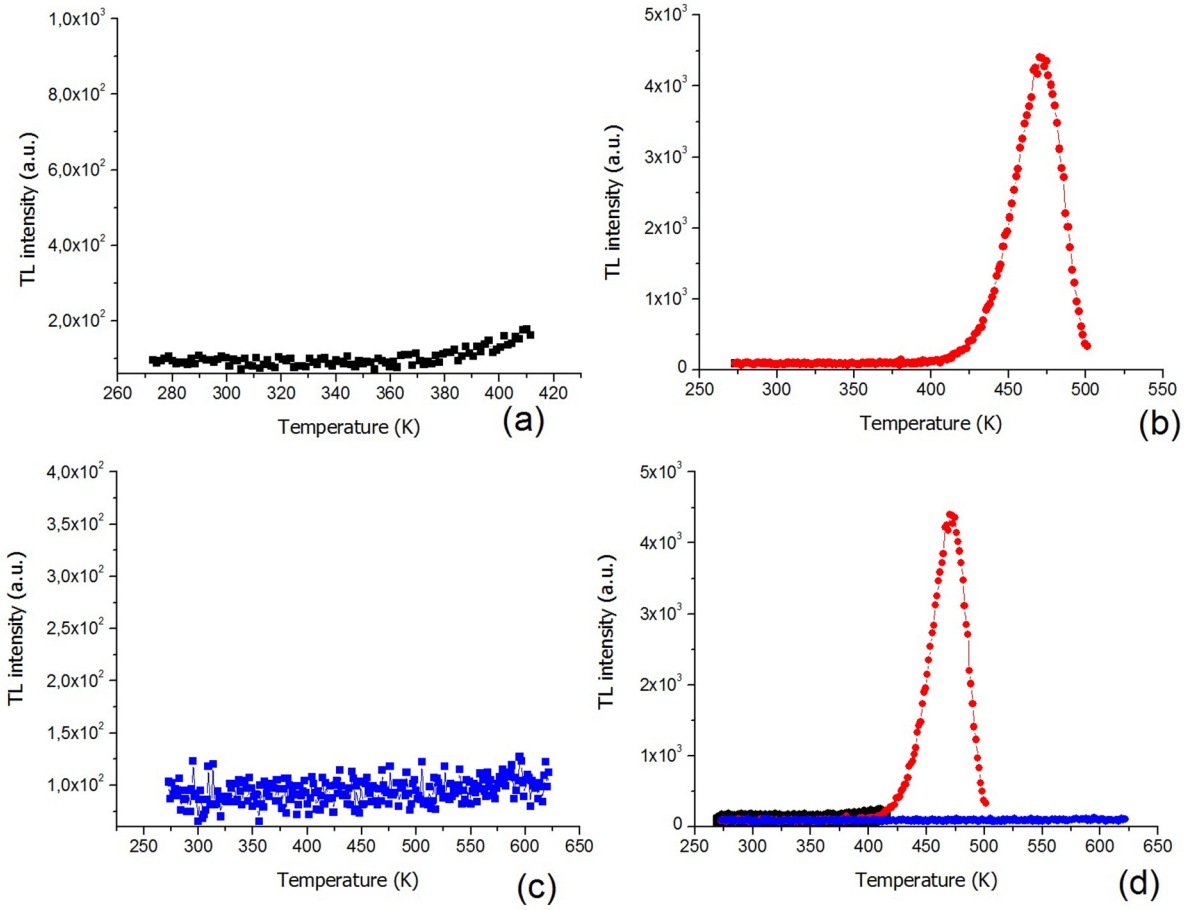

FIG. 7. Partial heating experiment: (a) The sample was partially heated up to 413 K, and then the glow curve was recorded; (b) the sample was partially heated up to temperature beyond the peak, and the glow curve was recorded; (c) the sample was heated up to 623 K, and the glow curve was recorded; (d) sum of all the curves. The dosimetric peak was around 470 K.

Figure 7 shows the presence of one dosimetric peak in the considered temperature range. The result is in agreement with the Akselrod and Akselrod (2002) work, where several crystals of the Landauer Inc., Stillwater Crystal Growth Division were studied, and the first group of them showed a normal, narrow, TL peak (main dosimetry peak). Whitley and McKeever (2002) showed "a sample-to-sample variability" in the TL measurement of Al_2O_3:C in experiments performed with samples obtained from either Landauer Inc. (Oklahoma, USA) or Bicron NE (Ohio, USA).

C. Determination of the number and position of TL peaks

For the determination of the number and position of the peaks, the (T_M–T_{stop}) analysis was utilized. The sample was irradiated to 0.5 Gy, and the established T_{stop} temperature for partial heating was 413 K. After this, the sample was cooled, and the complete glow curve was obtained. This analysis was repeated several times for the same sample, freshly irradiated each time, and the

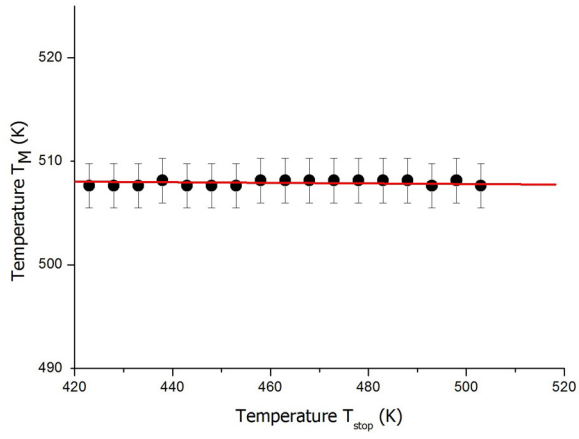

FIG. 8. (T_M–T_{stop}) curve of the SOL-GEL α-Al_2O_3 detectors.

T_{stop} temperature was varied in increments of 5 K from 413 K up to 503 K. Figure 8 shows the (T_M–T_{stop}) curve. This curve is a line taking into account the uncertainties of the different points. It is evident that T_M is independent of T_{stop}. This feature suggests that the peak is free of overlapping components. Figure 8 shows that there is a single peak in the glow curve.

D. Assessment for the order of kinetics

To assess the order of kinetics of the SOL-GEL α-Al_2O_3 peak detectors, the T_M-dose method was used. Figure 9 shows the glow curves measured at 5 K/s after irradiation to different doses of the $^{90}Sr/^{90}Y$ and ^{85}Kr sources of the Beta Secondary Standard 2 (BSS2) and the variation of the temperature peak position as a function of the absorbed dose. The peak temperatures are 500 ± 2 K and 511 ± 2 K for the $^{90}Sr/^{90}Y$ and ^{85}Kr sources, respectively. The peaks are similar in the irradiation dose range; therefore, it can be considered that the peaks are of first order kinetics. A strong energy dependence of these detector responses was observed in relation to the beta radiation energy of the BSS2 system (Polo and Caldas, 2019).

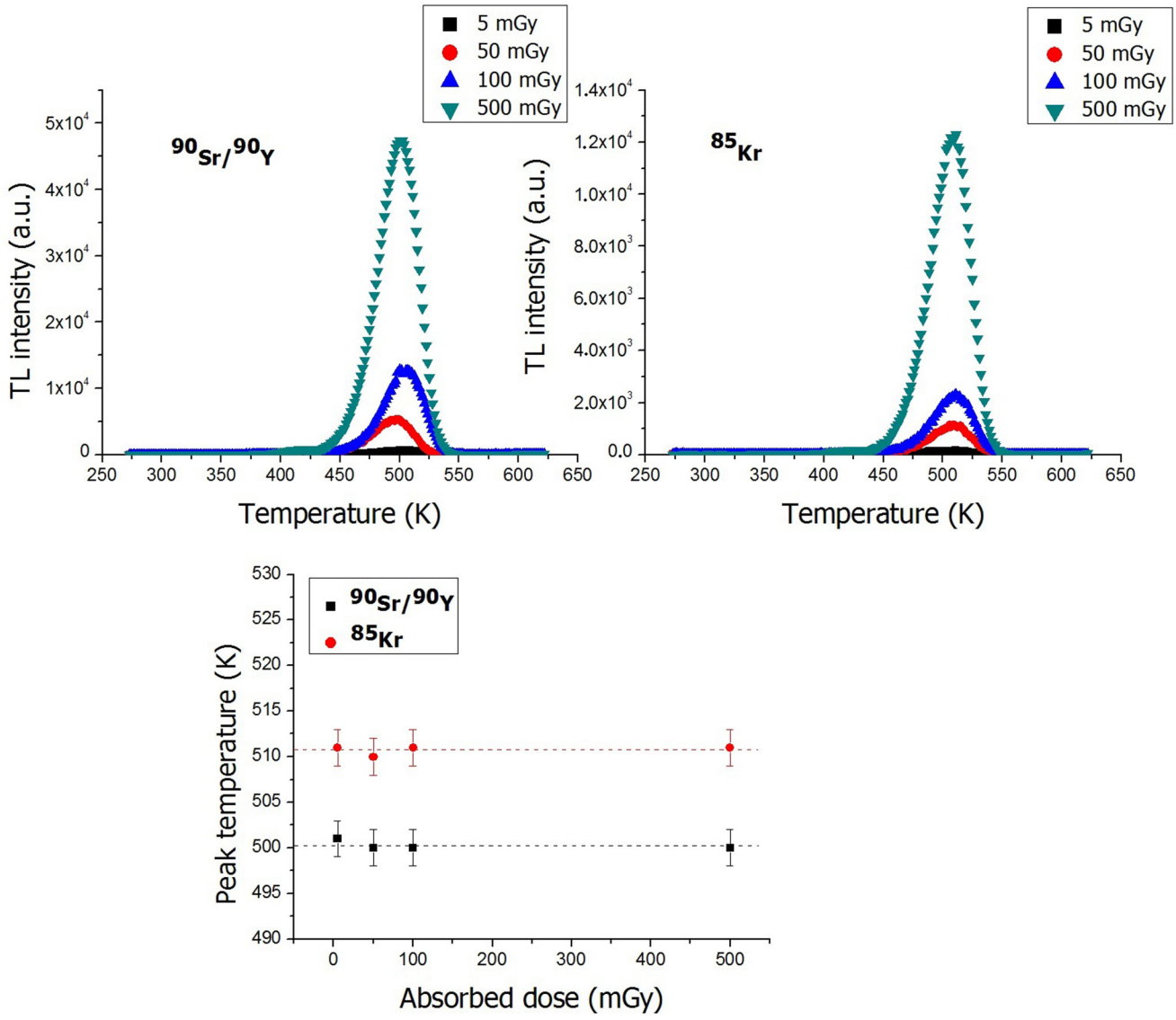

FIG. 9. Glow curves measured at 5 K/s after irradiation to different doses of the $^{90}Sr/^{90}Y$ and ^{85}Kr BSS2 sources and the variation of the temperature peak position as a function of the absorbed dose.

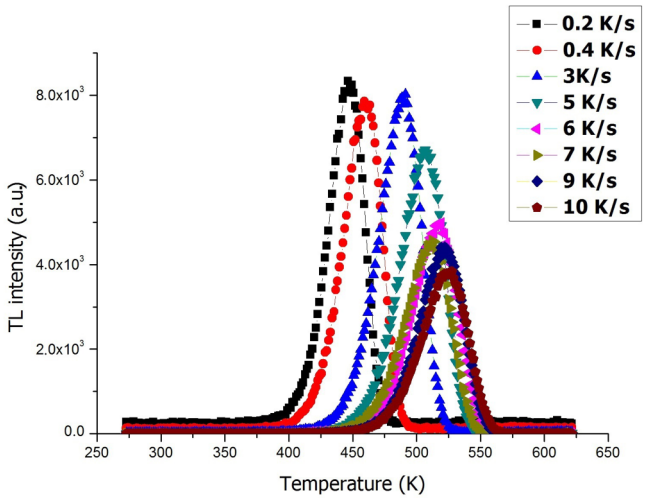

FIG. 10. TL glow curves of the α-Al_2O_3 SOL-GEL detectors obtained at different heating rates, after irradiation with the RISØ TL/OSL-DA20 $^{90}Sr/^{90}Y$ source.

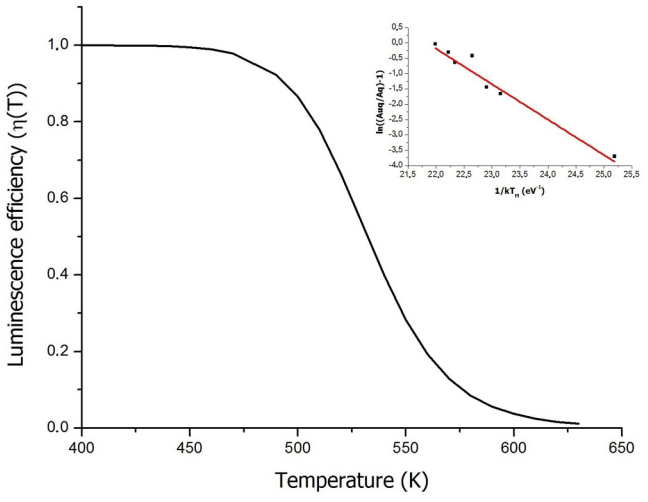

FIG. 11. Efficiency of luminescence as a function of temperature. Curve obtained using the parameters W = 1.15 ± 0.15 eV and C = 8.27 × 10^{10} s^{-1}. The inset shows the plot of $[(A_{uq}/A_q) - 1]$ vs $1/kT_M$ used to evaluate the quenching parameters.

E. Analysis of thermal quenching

Knowing that the thermal quenching occurs in aluminum oxide, this effect was evaluated. In the absence of thermal quenching, the area below the glow peak curve must be constant regardless of the heating rate. Figure 10 shows the TL glow curves of the SOL-GEL α-Al_2O_3 detectors obtained at different heating rates after irradiation to 0.5 Gy of the RISØ TL/OSL-DA20 $^{90}Sr/^{90}Y$ source.

In Fig. 10, a decrease of the area of the glow peak can be observed with the increase of the heating rate. This is the case for thermal quenching (Kitis, 2002; Pagonis *et al.*, 2006; and Kalita and Chithambo, 2017a). The activation energy of thermal quenching can be determined by Eq. (15). Based on the glow curves measured with different heating rates in Fig. 10, it can be assumed that the emission curve measured at 0.2 K/s is not affected by the thermal quenching effect.

Parameters W = 1.05 ± 0.15 eV and C = 8.27 × 10^{10} s^{-1} were estimated from the angular coefficient and the linear curve fit intercept of the graph $\ln[(A_{uq}/A_q)-1]$ vs $1/kT_M$. Akselrod *et al.* (1998) obtained that W is between 1.04 and 1.09 eV, and Ogundare *et al.* (2013) reported W = 0.96 ± 0.05 eV for the α-Al_2O_3:C material. Kalita and Chithambo (2017a) reported values of W = 0.99 ± 0.08 eV and C = 5.95 × 10^{10} s^{-1} for the α-Al_2O_3:C,Mg material. The values determined in this work are similar to those obtained by these authors. From the values of W and C it is possible to obtain the efficiency curve of the luminescence. Figure 11 shows a plot of the efficiency of luminescence as a function of temperature. In the inset of Fig. 11, the plot of $[(A_{uq}/A_q)-1]$ vs $1/kT_M$ is shown.

From Fig. 11, it can be seen that the efficiency of the luminescence is equal to 1 for temperatures up to approximately 475 K. Above this temperature, the efficiency becomes lower than 1, and it decreases dramatically as the temperature increases. The temperature of 475 K can be considered as critical to determine the activation energy, because below that temperature, the efficiency of the luminescence is equal to 1, and there is no effect of thermal quenching yet. According to Chithambo (2014), the theoretical limit of W in α-Al_2O_3:C cannot exceed 3 eV.

F. Methods for determination of kinetic parameters

For the determination of the kinetic parameters, a heating rate of 0.2 K/s was chosen where the efficiency of the luminescence is equal to 1, and the peak temperature is not affected by the thermal quenching.

For the first approximation of the activation energy values, the Randall and Wilkins and Urbach methods (Pagonis *et al.*, 2006) were used.

For the peak shape methods, the temperature values were as follows: T_1 = 424.35 K; T_2 = 463.15 K, and T_M = 447 K. The parameters determined based on the peak shape of the TL glow curve (see Fig. 1) are shown in Table I. According to this method, the value of μ = 0.42 indicates a first order peak.

For the methods using the TL glow curve area, the integral of the peak area curve was determined using the sum of the curve values from the temperature 375 K to 455 K. According to Eq. (13), the sum of this values must be multiplied by the temperature interval (ΔT = 1 K), and divided by the heating rate (β = 0.2 K/s). Figure 12 shows the curves of $\ln(TL/Area^b)$ vs $1/kT$ for the following kinetic order values b = 1; b = 1.1; and b = 1.2.

TABLE I. Parameters for methods based on the peak shape of the TL glow curve.

τ (K)	δ (K)	ω (K)	μ
22.4 ± 5.7	16.4 ± 5.7	38.8 ± 5.7	0.42 ± 0.16

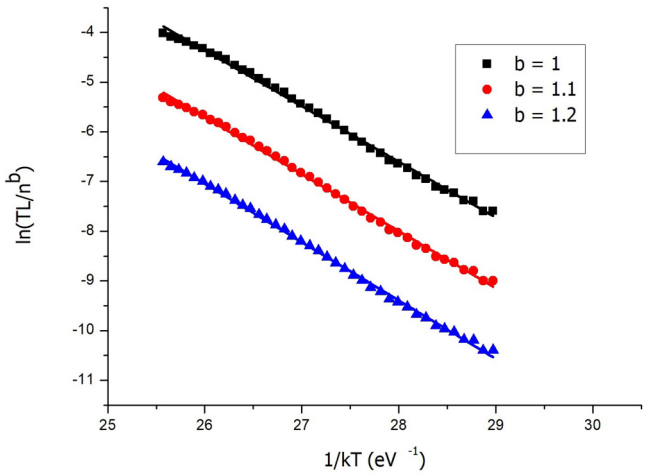

FIG. 12. Curves of ln (TL/n^b) vs 1/kT for several values of the kinetic order b.

The correlation coefficients R^2 for the curves following the least-square linear fitting were as follows: 0.99053; 0.99011; and 0.98945 for b = 1; b = 1.1; and b = 1.2, respectively. It can be observed that the curve of the best fit was that corresponding to b = 1. The angular coefficient was −1.038 ± 0.014 eV, and the intercept was 22.5 ± 0.4.

The peak was analyzed by the computer program Glow Fit. The peak temperature values and peak intensity were $T_M = 447$ K and $I_M = 8335$, respectively. Figure 13 shows the TL glow curve with the best fit. The fit residuals are shown, and they fluctuated around zero confirming the goodness of the fit. The best fit with FOM = 0.8 leads to an activation energy of E = 0.998 ± 0.020 eV.

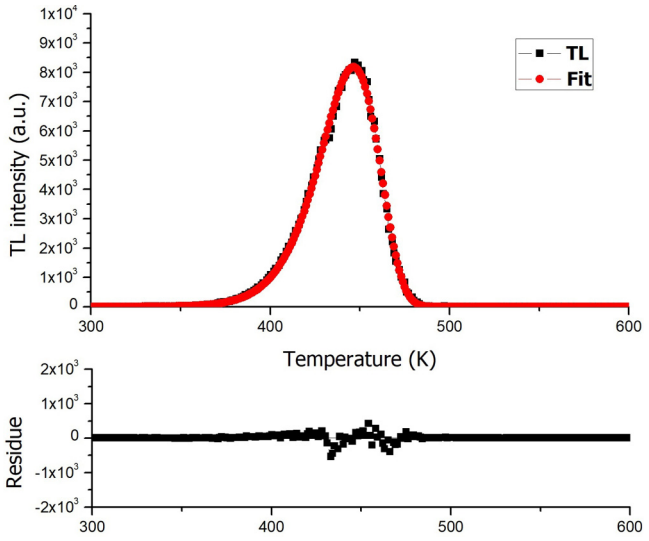

FIG. 13. Curve deconvolution for the peak of SOL-GEL α-Al_2O_3 detectors obtained with the computer program Glow Fit. The fit residuals confirm the goodness of the fit.

Table II summarizes the values obtained for the activation energy and the frequency factor of trapping states involved in the TL emission for the SOL-GEL α-Al_2O_3 material determined by different methods. Table II also includes average values with uncertainties for the activation energy and the frequency factor.

It can be concluded that the peak of SOL-GEL α-Al_2O_3 follows first order kinetics. Kalita and Chithambo (2017a) reported the first order kinetic peak for the main glow peak in α-Al_2O_3:C:Mg.

The values of the parameters obtained by the method of the peak shape of the glow curve were in agreement and within the uncertainty range. The activation energy value for the curve peak area method is in accordance with the above methods and within the uncertainty range. The values of the parameters obtained by fitting the curves using the Glow Fit computer program are also in agreement with the values of the cited methods. For α-Al_2O_3:C activation energy mean values of 0.97 ± 0.03 eV for the whole glow peak method and 0.96 ± 0.08 eV for the peak shape method were reported (Ogundare *et al.*, 2013). For α-Al_2O_3:C,Mg, the activation energy values of ∼0.83 eV, 0.96 eV, 1.37 eV, 1.20 eV, 1.15 eV, 1.61 eV, and 1.94 eV for peaks I through VII, respectively, were reported, and the frequency factors for all the peaks were of the order of 10^9–10^{14} s^{-1} (Kalita and Chithambo, 2017b).

Table III shows a comparison of some TL characteristics of Al_2O_3 based commercially materials prepared by different methods (Bhatt and Kulkarni, 2014). Table III also includes the characteristics of the SOL-GEL α-Al_2O_3 detectors.

Table III reveals that the crystals can exhibit a different glow curve due to the nature of their preparation and impurities.

TABLE II. Activation energy and frequency factor for the SOL-GEL α-Al_2O_3 material.

Methods	Activation energy (eV)	Frequency factor (s^{-1})
Randall and Wilkins	0.962 ± 0.009	2×10^9
Urbach	0.885 ± 0.008	10^9
Chen τ	1.04 ± 0.29	$(6.1 \pm 0.5) \times 10^9$
Chen δ	1.02 ± 0.38	$(4.2 \pm 0.4) \times 10^9$
Chen ω	1.04 ± 0.16	$(6.54 \pm 0.29) \times 10^9$
Grossweiner	1.03 ± 0.31	$(4.8 \pm 0.4) \times 10^9$
Lushchik	1.02 ± 0.38	$(4.2 \pm 0.4) \times 10^9$
Halperin and Braner	1.05 ± 0.10	$(7.55 \pm 0.20) \times 10^9$
Balarin	1.03 ± 0.15	$(4.8 \pm 0.4) \times 10^9$
TL glow curve peak area	1.038 ± 0.014	$(1.23 \pm 0.12) \times 10^9$
Curve deconvolution by the Glow Fit program	0.998 ± 0.020	2.10×10^9
Average values[a]	1.025 ± 0.011	$(1.24 \pm 0.12) \times 10^9$

[a]These values were obtained by calculating the average of the activation energies and the frequency factors determined through all the methods, except the Randall and Wilkins, and the Urbach methods.

TABLE III. Comparison of TL characteristics of Al_2O_3 based materials prepared by different methods (Bhatt and Kulkarni, 2014) and SOL-GEL α-Al_2O_3 detectors.

Physical form and method of preparation	Main TL peak (K)	TL sensitivity	TL emission (nm)	Dose response (region of linearity)
Al_2O_3:Si,Ti (300, 100 ppm) phosphor powder. Prepared by sintering in air by flame treatment (to about 2000 °C) (Mehta and Sengupta, 1976)	523 K (main TL peak), 748 K	5 times that of TLD-100	420 nm	523 K peak saturates at 3×10^2 Gy. Minimum detectable dose = a few tens of μGy
Al_2O_3:Mg,Y sintered pellets (8 mm diameter×1 mm thickness). Cold pressed pellets containing appropriate amounts of Mg and Y were sintered at 1600 °C in air (Osvay and Biro, 1981)	An intense dosimetric peak at ∼553 K, with a low intensity shoulder at ∼463 K at a heating rate of 10 °C/s	Not reported	440 nm, weak emission at 695 nm	0.1 mGy to a few kGy
Al_2O_3:Na, Ti (0.7, 4.0 mol. %) (Portal and Lorrain, 1980 and Portal, 1981)	538 K (main TL peak), 708 K, 908 K	Comparable to TLD-100	550 nm, 390 nm	5×10^{-2} to 10 Gy. Saturation at 10^3 Gy
Al_2O_3:Cr, Ni single crystals ($10 \times 10 \times 1$ mm^3). Grown by the Verneuil method (Pokorny and Ibarra, 1993)	603 K	150 times higher than that of TLD-100	695 nm	TL sensitivity comparison was done at an X-ray dose >10 Gy
α-Al_2O_3:C single crystals (5 mm diameter × 1 mm thickness). Using subtractive coloration technique (Akselrod *et al.*, 1990)	A single glow peak at 460 K	50 times higher than that of LiF:Mg,Ti	420 nm	Negligible fading
Al_2O_3 single crystals. Grown by the Czochralski method (Lucas and Lucas, 1999)	Five TL peaks in the range 90–673 K			623 K TL peak in Al_2O_3:Si, Useful response from 0.1 kGy to at least 10 kGy
SOL-GEL α-Al_2O_3 detectors (Ferreira and Santos, 2014)	One peak at ∼447 K 0.2 K/s	24 times higher than that of TLD-100	420 nm, 697 nm, 750 nm, 800 nm	Good linearity of response from 0.01 to 1000 mGy

Further investigation is necessary in order to study the temperature peaks at 697 nm, 750 nm, and 800 nm using other filters and to search for evidence if these peaks are suitable for radiation dosimetry.

IV. CONCLUSIONS

The analysis of the TL kinetic parameters of SOL-GEL α-Al_2O_3 was presented. The TL glow curve revealed one peak at around 447 K obtained after 0.5 Gy beta irradiation for 0.2 K/s of heating rate. The (T_M–T_{stop}) method was used for determination of the peak number, and the T_M dependence on the radiation dose method was used to assess the order of kinetics of the peak. The obtained results by these methods suggest that the peak follows first order kinetics. The analysis of the fractional glow curve method showed that there is just a single peak in the TL glow curve. TL spectra recorded at 5 K/s after beta irradiation revealed the peaks at approximately 420 nm, 700 nm, 750 nm, and 800 nm. The activation energies and the frequency factors were obtained by the maximum peak temperature response, the peak shape of the TL glow curve, the TL glow curve area, and the glow curve fitting methods. The activation energies calculated varied from 0.885 ± 0.008 eV to 1.05 ± 0.10 eV. The frequency factor was in all cases of the order of 10^9 s^{-1}. The activation energies and frequency factors determined by different used methods are in good agreement with one another. The peak is affected by thermal quenching. Above 475 K, the thermal quenching increases considerably.

ACKNOWLEDGMENTS

The α-Al_2O_3 detectors were gently offered by Dr. Hudson Ferreira from the Centro de Desenvolvimento da Tecnologia Nuclear (CDTN/CNEN), Brazil, to whom the authors are very grateful. The authors also acknowledge the partial financial support of the Brazilian Funding Agencies CNPq (Project No. 142297/2015-1, fellowship of I. O. Polo; and 301335/2016-8), FAPESP (Project No. 2008/57863-2), and MCTIC: INCT Project: Radiation Metrology in Medicine (Project No. 573659/2008-7).

REFERENCES

Akselrod, M. S., Agersnap Larsen, N., Whitley, V., and McKeever, S. W. S., "Thermal quenching of F-center luminescence in Al_2O_3:C," J. Appl. Phys. **84**, 3364–3373 (1998).

Akselrod, M. S. and Akselrod, A. E., "Correlation between OSL and the distribution of TL traps in Al_2O_3:C," Radiat. Prot. Dosim. **100**(1–4), 217–220 (2002).

Akselrod, M. S. and Akselrod, A. E., "New Al_2O_3:C,Mg crystals for radiophotoluminescent dosimetry and optical imaging," Radiat. Prot. Dosim. **119**(1–4), 218–221 (2006).

Akselrod, M. S., Bøtter-Jensen, L., and McKeever, S. W. S., "Optically stimulated luminescence and its use in medical dosimetry," Radiat. Meas. **41**, S78–S99 (2006).

Akselrod, M. S., Kortov, V. S., Kravestky, D. J., and Gotlib, V. I., "Highly sensitive thermoluminescent anion-defective α-Al_2O_3:C single crystal detectors," Radiat. Prot. Dosim. **32**(1), 15–20 (1990).

Bao, A., Tao, C., and Yang, H., "Synthesis and luminescent properties of nanoparticles $GdCaAl_3O_7$:RE3+ (RE=Eu, Tb) via the sol–gel method," J. Lumin. **126**, 859–865 (2007).

Bhatt, B. C. and Kulkarni, M. S., "Thermoluminescent phosphors for radiation dosimetry," Defect Diffus. Forum **347**, 179–227 (2014).

Bitencourt, J. F. S., Ventieri, K., Gonçalves, K. A., Pires, E. L., Mittani, J. C., and Tatumi, H. A., "Comparison between neodymium doped alumina samples obtained by Pechini and sol-gel methods using thermo-stimulated luminescence and SEM," J. Non-Crystal **356**, 2956–2959 (2010).

Bos, A. J. J., "Thermoluminescence as a research tool to investigate luminescence mechanisms," Materials **10**, 1357 (2017).

Bouman, J. "On the deep-red luminescence of Cr^{3+} in $Y_3Al_{5-x}Ga_xO_{12}$:Cr^{3+}," M.Sc. thesis (Ghent University, Belgium, 2016).

Brinker, C. J. and Scherer, G. W., *Sol-Gel Science: The Physics and Chemistry of Sol-Gel Processing* (Academic Press Inc., San Diego, 1990).

Caiut, J. M. A., Floch, N., Messaddeq, Y., de Lima, O. J., Rocha, L. A., Ciuffi, K. J., Nassar, E. J., Friedermannd, G. R., and Ribeiro, S. J. L., "Cr^{3+} doped Al_2O_3 obtained by non-hydrolytic sol-gel methodology," J. Braz. Chem. Soc. **3**(4), 744–751 (2019).

Chen, R. and Kirsh, Y., *The Analysis of Thermally Stimulated Processes*, International Series in the Science of the Solid State Vol. 15 (Pergamon, 1981), pp. 17–59.

Chen, R. and McKeever, S. W. S., *Theory of Thermoluminescence and Related Phenomena* (World Scientific, Singapore, 1997).

Chen, R. and Pagonis, V., "Study of the stability of the TL and OSL signals," Radiat. Meas. **81**, 192–197 (2015).

Chen, R., Pagonis, V., and Lawless, J. L., "Evaluated thermoluminescence trapping parameters—What do they really mean?," Radiat. Meas. **91**, 21–27 (2016).

Chithambo, M. L., "A method for kinetic analysis and study of thermal quenching in thermoluminescence based on use of the area under an isothermal decay-curve," J. Lumin. **151**, 235–243 (2014).

De Azevedo, W. M., de Oliveira, G. B., da Silva, E. F., Jr., Khoury, H. J., and Oliveira de Jesus, E. F., "Highly sensitive thermoluminescent carbon doped nanoporous aluminium oxide detectors," Radiat. Prot. Dosim. **119**, 201–205 (2006).

DTU Nutech, *Guide to "The Risø TL/OSL Reader"* (DTU Nutech, Denmark, 2015).

Ferreira, H. R. and Santos, A., "Preparation and characterization of a SOL-GEL α-Al_2O_3 polycrystalline detector," Radiat. Prot. Dosim. **163**, 166–172 (2014).

Furetta, C., *Handbook of Thermoluminescence* (World Scientific Publishing, Singapore, 2003).

Furetta, C., *Questions and Answers on Thermoluminescence (TL) and Optically Stimulated Luminescence (OSL)* (World Scientific Publishing, London, 2008).

Furetta, C. and Weng, P., *Operational Thermoluminescence Dosimetry* (World Scientific Publishing, Singapore, 1998).

Gaft, M., Reisfield, R., and Panczer, G., *Modern Luminescence Spectroscopy of Minerals and Materials* (Springer, Cham, 2015).

Jalali, M. R., "Improvement of thermoluminescence properties of α-Al_2O_3 using metallic dopants for dosimetry application," Int. J. Env. Sci. Educ. **13**, 229–236 (2018).

Kalita, J. M. and Chithambo, M. L., "Thermoluminescence of α-Al_2O_3:C,Mg: Kinetic analysis of the main glow peak," J. Lumin. **182**, 177–182 (2017a).

Kalita, J. M. and Chithambo, M. L., "Comprehensive kinetic analysis of thermoluminescence peaks of α-Al_2O_3:C,Mg," J. Lumin. **185**, 72–82 (2017b).

Kitis, G., "TL glow curve deconvolution functions for various kinetic orders and continuous trap distribution: Acceptance criteria for E and s values," J. Radioanalyt. Nucl. Chem. **247**, 697–703 (2001).

Kitis, G., "Confirmation of the influence of thermal quenching on the initial rise method in α-Al_2O_3:C," Phys. Status Solidi A **191**, 621–627 (2002).

Kitis, G., Gomez-Ros, J. M., and Tuyn, J. W. N., "Thermoluminescence glow curve deconvolution functions for first, second and general orders of kinetics," J. Phys. D Appl. Phys. **31**, 2636–2641 (1998).

Lu, S., Chunfeng, H., Shenghu, Z., Amiya, M., and Qing, H., "Phase-dependent photoluminescence behavior of Cr-doped alumina phosphors," Opt. Mater. **35**, 1268–1272 (2013).

Lucas, A. C. and Lucas, B. K., "High dose TL response of Al_2O_3 single crystals," Radiat. Prot. Dosim. **85**, 455–458 (1999).

McKeever, S. W. S., *Thermoluminescence of Solids*, Cambridge Solid State Science Series (Cambridge University Press, Cambridge, 1985).

McKeever, S. W. S., "On the analysis of complex thermoluminescence glow curves: Resolution into individual peaks," Phys. Status Solidi A **62**, 331–340 (1980).

Mehta, S. K. and Sengupta, S., "Gamma dosimetry with Al_2O_3 thermoluminescent phosphor," Phys. Med. Biol. **21**, 955–964 (1976).

Nyirenda, A. N. and Chithambo, M. L., "Spectral study of radioluminescence in carbon-doped aluminium oxide," Radiat. Meas. **120**, 89–95 (2018).

Ocean Optics QE65 Pro Data Sheet, see http://www.OceanOptics.com, 2018.

Ogundare, F. O., Ogundele, S. A., Chithambo, M. L., and Fasasi, M. K., "Thermoluminescence characteristics of the main glow peak in α-Al_2O_3:C exposed to low environmental-like radiation doses," J. Lumin. **139**, 143–148 (2013).

Osvay, M. and Biro, T., "Aluminium oxide," in *Applied Thermoluninescence Dosimetry*, edited by M. Oberhofer and A. Scharmann (Adam Hilger, Bristol, 1981), pp. 243–263.

Pagonis, V., Ankjærgaard, C., Murray, A. S., Jain, M., Chen, R., Lawless, J., and Greilich, S., "Modelling the thermal quenching mechanism in quartz based on time-resolved optically stimulated luminescence," J. Lumin. **130**, 902–909 (2010).

Pagonis, V., Kitis, G., and Furetta, C., *Numerical and Practical Exercises in Thermoluminescence* (Springer Science + Business Media, New York, 2006).

Pierre, A. C., *Introduction to Sol-Gel Processing* (Kluwer Academic Publishers, New York, 1998).

Pokorny, P. and Ibarra, A., "On the origin of the thermoluminescence of Al_2O_3: Cr,Ni," J. Phys. Condens. Matter **5**, 7387–7396 (1993).

Polo, I. O. and Caldas, L. V. E., "SOL-GEL α-Al_2O_3 detectors: TL and OSL response to beta radiation beams," Radiat. Phys. Chem. (in press).

Portal, G., "Preparation and properties of principal TL products," in *Applied Thermoluninescence Dosimetry*, edited by M. Oberhofer and A. Scharmann (Adam Hilger, Bristol, 1981), pp. 97–122.

Portal, G. and Lorrain, S., "Very deep traps in Al_2O_3 and $CaSO_4$:Dy," Nucl. Instrum. Methods **175**, 12–14 (1980).

Puchalska, M. and Bilski, P., "GlowFit—A new tool for thermoluminescence glow-curve deconvolution," Radiat. Meas. **41**(6), 659–664 (2006).

Rivera, T., "Synthesis and thermoluminescent characterization of ceramics materials," in *Advances in Ceramics—Synthesis and Characterization, Processing and Specific Applications*, see https://www.intechopen.com/books (2011).

Rivera, T., Azorin, J., Barrera, M., Soto, A. M., and Furetta, C., "Thermoluminescence (TL) of europium-doped ZrO_2 obtained by sol-gel method," Radiat. Eff. Def. Sol. **162**(5), 378–383 (2007a).

Rivera, T., Azorín, J., Barrera, M., and Soto, A. M., "Nanostructural processing of advanced thermoluminescent materials," Radiat. Eff. Def. Sol. **162**, 731–736 (2007b).

Rivera, T., Olvera, L., Azorin, J., Sosa, R., Soto, A. M., Barrera, M., and Furetta, C., "Preparation of luminescent nanocrystals started from amorphous zirconia prepared by sol-gel technique," Radiat. Eff. Def. Sol. **161**(2), 91–100 (2006).

Rivera, T., Sosa, T., Azorín, J., Zarate, J., and Ceja, A., "Synthesis and luminescent characterization of sol-gel derived zirconia-alumina," Radiat. Meas. **45**, 465–467 (2010).

Rodriguez, M. G., Denis, G., Akselrod, M. S., Underwood, T. H., and Yukihara, E. G., "Thermoluminescence, optically stimulated luminescence and radioluminescence properties of Al_2O_3:C,Mg," Radiat. Meas. **46**(12), 1469–1473 (2011).

Rotman, S. R., Warde, C., Tuller, H. L., and Haggerty, J., "Defect-property correlations in garnet crystals. V. Energy transfer in luminescent yttrium aluminum–yttrium iron garnet solid solutions," J. Appl. Phys. **66**(7), 3207–3210 (1989).

Valle, J. F., Garcia-Guinea, F., and Correcher, J. V., "Espectros de emisión de radioluminiscencia y termoluminiscencia de una leucita de Monte Somma (Italia)," Bol. Soc. Esp. Ceram. **43**, 919–924 (2004).

Varney, C. R., Reda, S. M., Mackay, D. T., Rowe, M. C., and Selim, F. A., "Strong visible and near infrared luminescence in undoped YAG single crystals," AIP Adv. **1**, 042170-1–042170-6 (2011).

Whitley, V. H. and McKeever, S. W. S., "Linear modulation optically stimulated luminescence and thermoluminescence techniques in Al_2O_3:C," Radiat. Prot. Dosim. **100**(1–4), 61–66 (2002).

Yoshizumi, M. T. and Caldas, L. V. E., "TL emission spectra measurement using a spectrometer coupled to the Risoe TL/OSL reader," Radiat. Phys. Chem. **104**, 292–296 (2014).

Yukihara, E. G., Whitley, V. H., Polf, J. C., Klein, D. M., McKeever, S. W. S., Akselrod, A. E., and Akselrod, M. S., "The effects of deep trap population on the thermoluminescence of Al_2O_3:C," Radiat. Meas. **37**, 627–638 (2003).